

## Formation of Poly(vinylidene fluoride) Nanofibers

### Part II: the elaboration of incompatibility in the electrospinning of its solutions

Ahmad Akbari<sup>\*a,b</sup>, Arash Yunessnia lehi<sup>b</sup>

<sup>a</sup> Department of Carpet, Faculty of Architecture & Art, University of Kashan, Kashan, Iran

<sup>b</sup> Institute of Nanoscience and Nanotechnology, University of Kashan, Kashan, Iran

#### Article history:

Received 13/5/2012

Accepted 18/8/2012

Published online 1/9/2012

#### Keywords:

Crystallization

Electrospinning Process

Microgels

Poly(vinylidene fluoride)

Solution Entanglement Number

Spinodal Decomposition

#### \*Corresponding author:

E-mail address:

akbari@kashanu.ac.ir

Phone: +98 361 5913154

Fax: +98 361 5913131

P.O. Box: 87317-51167

#### Abstract

Poly(vinylidene fluoride) (PVDF) fibers with two molecular weights were prepared via electrospinning process. In this process, the concentration of spinning depended drastically on the gelation process. Also, it was experimentally smaller than obtained concentration in the solution entanglement number approach (SENA). Proof of this incompatibility was explained by the properties of PVDF and its solutions with DMF (i.e. PVDF crystallization, microgel formation and spinodal decomposition). These factors caused to early stabilize liquid jet. Also, early gelation inhibited from the fiber formation by blockage of syringe needle with  $M_w = 180,000$  g/mol and early spinodal decomposition helps to fiber formation by isolated droplets of polymer-rich phase with  $M_w = 275,000$  g/mol. Finally, a mechanism was proposed for the electrospinning of these solutions.

2012 JNS All rights reserved

### 1. Introduction

Most of the researchers considered the applications of electrospun fibers. Recently, the concerted efforts have been accomplished to gain deeper insights into the electrospinning process [1-3]. But, there is a lack of knowledge with regards to fiber formation and its relationship to the polymer solution properties. One of these solution parameters that more significantly affects the

electrospinning process is polymer concentration. Shenoy et al. introduced a semi-empirical methodology (solution entanglement number approach, SENA) to a priori predict the transition from electro spraying and electrospinning in good solvents [1]. In a good solvent, the electrostatic forces between repeat units of the polymer and solvent are favorable i.e. intermolecular forces between solvent and monomer subunits dominate

over intramolecular interactions. The polymer appears swollen and occupies a large volume. In their model, they defined solution entanglement number  $(n_e)_s$  as ratio of polymer weight average molecular weight ( $M_w$ ) to entanglement molecular weight in solution  $(M_e)_s$ .

$$(n_e)_s = \frac{M_w}{(M_e)_s} = \frac{\phi M_w}{(M_e)_m}$$

Here,  $(M_e)_m$  is entanglement molecular weight in the melt and  $\phi$  is polymer volume fraction. Note that an underlying assumption of this approach is that chain entanglements are solely responsible for both initiation of fiber formation and continuous fiber formation under influence of an elongational strain. Therefore, this approach is valid only for good solvent case where polymer-polymer interactions are negligible [1]. But, the concentration and electrospinning of these solutions depends extremely on the gelation process [4-7]. Moreover, the type of gelation process differs in amorphous and semicrystalline polymer solutions [4, 5, 8, 9]. Therefore, the purpose of this research is to efficiently determine the effect of concentration in the semicrystalline polymers to achieve best mechanism in the formation of fibers. In order to consider and explain the electrospinnability, we used poly(vinylidene fluoride) [3, 8].

## 2. Experimental procedure

As received poly(vinylidene fluoride) granules (PVDF, Aldrich,  $M_w=180,000$ ,  $M_n=71,000$  g/mol and  $M_w=275,000$ ,  $M_n=107,000$  g/mol,  $d=1.74$  g/mL) were first dissolved in N, N-dimethylformamide (DMF, Merck,  $d=0.94$  g/mL) at various concentrations, 20-25% wt. for  $M_w=275,000$  and 24-37% wt. for  $M_w=180,000$ , and solution temperature of  $75\pm 2^\circ\text{C}$ . The solutions

were magnetically stirred for at least one day. After that, the electrospinning process was run and fibers were spun at flow rate of  $0.1\pm 0.05$  mL/h, applied voltage of  $15\pm 0.1$  kV. They were collected on grounded aluminum tulle with distance of  $20\pm 3$  cm and temperature of electrospinning of  $38\pm 2^\circ\text{C}$  [10]. The used electrospinning system in this research was a homemade system (Fanavaran Nano-Meghyas Co., Iran). The X-ray diffraction data were collected by positioning of PVDF gels on a sample holder mounted in the powder diffractometer with  $\text{Cu K}_\alpha$  radiation (Philips PW1820, Netherland).

PVDF microgels were determined visually by an optical microscope (Olympus BX51). The small pieces of sample were placed between a pair of microscope cover slips. To prevent DMF loss by evaporation, Teflon film of  $200\ \mu\text{m}$  thickness with a circle opening was inserted between the cover slips. The diameter of microgels was measured with an image analyzer (Microstructure Measurement software, Nahamin Pardazan Asia Co.). For membrane preparation, the prepared homogeneous solution was cast by using of a film applicator to  $350\ \mu\text{m}$  clearance gap on a glass plate substrate. The cast film was subsequently rested at temperature  $38\pm 2^\circ\text{C}$  and relative humidity of 23% to complete the phase separation, where evaporation of solvent (DMF) was induced [11]. The membrane surface and fibers were characterized by scanning electron microscopy (LEO 1455VP, England).

## 3. Results and discussion

In Figure 1, the solution entanglement number approach (SENA) is shown for PVDF solutions with each  $M_w$  (i.e. 180,000 and 275,000 g/mol) [1]. We must figure out that entanglement molecular weight in melt state  $(M_e)_m$  for PVDF polymer is

22,700 g/mol [12]. An advantage of this approach is that required parameter for predictions is only  $(M_e)_m$ . According to this approach, both concentration and  $M_w$  affect the number of chain entanglement in PVDF solutions. In a dilute solution, below the critical value (38.4% wt. for PVDF with  $M_w=180,000$  g/mol and 28.6% wt. for  $M_w=275,000$  g/mol), chain overlapping is absent. As a result, there are no chain entanglements. In this region, the surface tension is dominated and the resulting electroprocessed mats consists of beads only (i.e. electrospaying process). The initiation of fiber spinning is at concentrations of 38.4% wt. for  $M_w=180,000$  g/mol and 28.6% wt. for  $M_w=275,000$  g/mol (due to PVDF chain entanglements). As concentration increases, the number of chain entanglements also increases. Concentrations between 38.4-59.4% wt. for PVDF with  $M_w=180,000$  g/mol and 28.6-42.9% wt. for  $M_w=275,000$  g/mol, beaded-fibers are formed. In these regions, the numbers of entanglements are insufficiently. These entanglements do not stabilize the jet of PVDF solutions that are under influence of strong elongational flow field. Finally, a continuous and beads-free fiber is collected at concentrations 59.4% wt. for  $M_w=180,000$  g/mol and 42.9% wt. for  $M_w=275,000$  g/mol (due to the formation of an elastically deformable network).

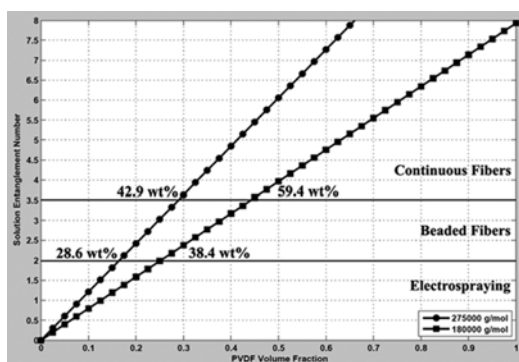


**Fig. 1.** Approach of solution entanglement number for PVDF solutions.

But, the concentration of continuous PVDF fiber formation differs experimentally with SENA's concentration. This approach ignores the interactions between polymer chains such as formation of hydrogen bonding and types of phase separation. In the electrospinning experiments for PVDF-DMF solutions, the initiation of fiber spinning was  $\sim 28\%$  wt. for  $M_w=180,000$  g/mol, whereas the continuous fibers were not obtained due to the extreme gelation and blockage of syringe. Also, the complete fibers were collected at  $\sim 20\%$  wt. for  $M_w=275,000$  g/mol. These concentrations are smaller than obtained concentrations in above approach. The proof of these differences can be explained with the properties of PVDF and its solutions with DMF.

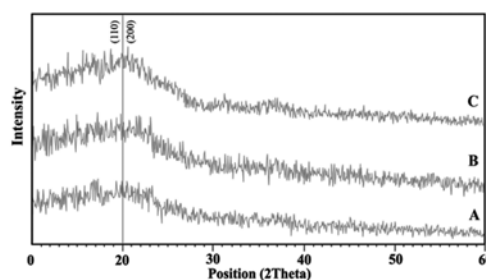


**Fig. 2.** XRD of PVDF gels with A: 20% wt.,  $M_w=275,000$  g/mol, B: 28% wt.,  $M_w=180,000$  g/mol and C: 33% wt.,  $M_w=180,000$  g/mol.

PVDF is a semicrystalline polymer and due to the presence of fluorine and hydrogen atoms, a weak interaction is probably formed between their chains. These interactions more drastically help to PVDF crystallization. This has been supported by extensive discussions on the gel melting behaviour [4, 5, 13]. The presence of a broad XRD peak at  $2\theta=20^\circ$  after a gelation time of more than 20 h confirms this reason (Fig. 2). This diffraction peak is assigned to the superposition of (110) and (200) diffractions from  $\beta$ -phase of PVDF crystallites. When PVDF concentration increases, the amount

of PVDF crystallization also increases. The formation of PVDF crystallites in the solutions earlier stabilizes the liquid jet.

Typical used methods to the synthesis of PVDF polymer often lead to short or long chain branches in their main chains (two molecular defects). It is well known that the branches strongly influence on the process ability of PVDF solutions. When the polydispersity index (PI) of PVDF polymer is above 2.5, we can result that chain branches exist in the chains [14]. The presence of these branches induces formation of microgel. In this research, PI of these received PVDF polymers was 2.54 and 2.57 for PVDF with  $M_w=180,000$  g/mol and 275,000 g/mol, respectively. We can obtain a good result that these solutions have few microgels. PVDF microgels were observed in this research by using of an optical microscope with high magnification. The size distribution of these microgels is as well shown in Figure 3. The size at the highest peaks was measured to be 0.86, 0.89 and 0.98  $\mu\text{m}$ . It provides a facile way to explain the electrospinning of PVDF-DMF solutions that microgels stabilize easier the ejected jet.

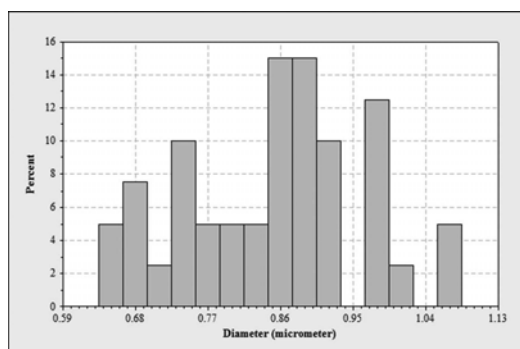


**Fig. 3.** Size distribution of PVDF microgels for  $M_w=275,000$  g/mol and 30% wt.

PVDF-DMF solutions are ready to form thermoreversible gels on cooling to room temperature within a few hours [8, 15]. The gel formation occurs due to the hydrogen bonding

between DMF molecules and PVDF chains and can affect the electrospinnability to a great degree [1]. Besides, the different types of phase separation take place in PVDF solutions [6, 8, 15]. We suggest that gelation is also induced by spinodal decomposition into the polymer-rich and polymer-poor regions [4, 5, 7, 15-17]. The verification of this case can be achieved by a convenient and effective procedure. For this matter, PVDF membranes were prepared by dry phase separation in the same electrospinning conditions (without applying of charge and electric field) and their surface was considered [11]. In the process of membrane formation, DMF from the cast film is evaporated by effecting of temperature and increasing non-solvent concentration (air) induces the phase separation of PVDF solution into a polymer-rich and a polymer-poor phase. Further evaporation of DMF will lead to an increase of the concentration and to vitrification of PVDF.

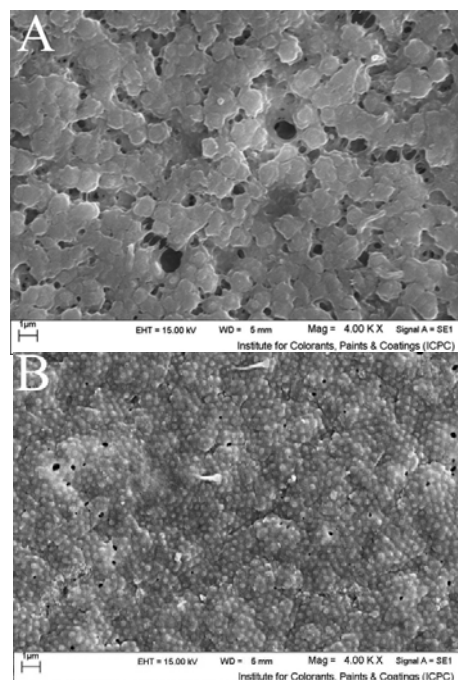


**Fig. 4.** SEM images of PVDF membrane surface at different concentrations (A: 20% wt. and B: 30% wt.) for  $M_w=275,000$  g/mol.

Accordingly, nodular structures existed in the membrane surface as shown in Figure 4 [17-19]. The nodules that normally characterize all PVDF membranes exhibit a range of sizes and compactness. Specifically, an increase in the concentration of casting solutions results in the increase of number and reduction of size. Generally, these nodules are formed by spinodal decomposition [17, 20]. As coarsening proceeds, the interfacial energy considerations drive the spheroidization of these material regions, which are ultimately integrated as nodules on the membrane surface. This phase separation is also confirmed by concentration-temperature phase diagram of PVDF solutions (Figure 5). This phase diagram was computed by the use of Liao-Ping Cheng's model [15] and was similar for each  $M_w$ . It can be stated that they drastically help to the electrospinning of PVDF solutions. This observation results in the temperature-sensitive solutions and a sol-gel transition [4, 6, 7].

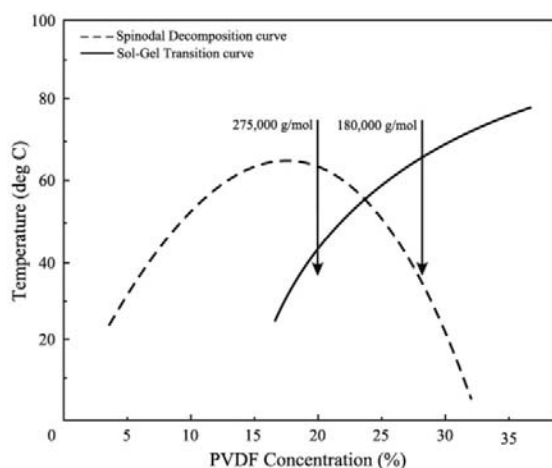


**Fig. 5.** Concentration-Temperature phase diagram of PVDF-DMF solutions.

Based on these results, we will explain the mechanism of PVDF fiber formation as shown in Figure 5. In the case of PVDF with  $M_w=180,000$  g/mol, solution is initially gelled by percolation

through hydrogen bonding (due to the temperature reduction from 75 to 38°C). PVDF concentration in DMF solvent is high, because of lower molecular weight. It should be affirmed that electrospinning process does not occur with dilute solutions of this  $M_w$ . Later, the network chains are organized into the crystallites to form a fringed-micelle type network swollen with DMF. Finally, the spinodal decomposition follows. It is confirmed by XRD data (Figure 2) [4-6, 13]. The amount of crystallites and their formation rate is low for the initiation of fiber spinning (i.e. beaded fiber) and these help to the electrospinning. But, this gelation prevents the formation of a continuous fiber in the beginning of electrospinning due to high concentration and thus, blockage occurs in the metal syringe needle.

In PVDF solutions with  $M_w=275,000$  g/mol, spinodal decomposition takes place that is a fast process. However, solution fails to change to a gel, because the connectivity of polymer-rich region is interrupted, resulting in isolated droplets of polymer-rich phase. This is as the result of small volume fraction of polymer-rich phase [7, 16]. The development of polymer-rich and polymer-poor and microgels in the solution helps to fiber formation via electrospinning process. Then, gelation in the polymer-rich region follows due to the solvent evaporation that causes to obtain a solid fibrous mat [6]. Of course, a complete gelation occurs at the higher concentrations.

#### 4. Conclusion

In this research, an attempt has been made to explain the influences of concentration and obtain a mechanism in PVDF (as semicrystalline polymer) fiber formation and electrospinning process. Two molecular weights were used for this polymer i.e. 180,000 and 275,000 g/mol. We

understand that three factors are resulted from concentration effects i.e. PVDF crystallization, microgel formation and spinodal decomposition that causes to stabilize the liquid jet in the electrospinning process and obtain fibers at lower concentrations. For the stabilization, they huddle some segments of PVDF polymer chains and make inflexible contacts. This produced network influences more significantly on the fiber development and hinders from breaking of fiber in the electrospinning process. It should be taken into consideration that amount of each factor is sufficiently. High amount of these factors in solution causes to gel and blockage of polymer solutions. The reason of incompatibility between solution entanglement number approach and these experiments was carefully described by a mechanism for each  $M_w$ . The SENA does not take into account these factors. Understandably, early gelation inhibited from the fiber formation by blockage of syringe needle with  $M_w=180,000$  g/mol and early spinodal decomposition helps to fiber formation by isolated droplets of polymer-rich phase with  $M_w=275,000$  g/mol.

## References

- [1] S.L. Shenoy, W.D. Bates, H.L. Frisch, G.E. Wnek, *Polymer*. 46 (2005) 3372-3384.
- [2] G.C. Rutledge, S.V. Fridrikh, *Adv. Drug Delivery Rev.* 59 (2007) 1384-1391.
- [3] M. Nasir, H. Matsumoto, T. Danno, M. Minagawa, T. Irisawa, M. Shioya, A. Tanioka, *J. Polym. Sci. B: Polym. Phys.* 44 (2006) 779-786.
- [4] J.H. Choi, S.W. Ko, B.C. Kim, J. Blackwell, W.S. Lyoo, *Macromolecules*. 34 (2001) 2964-2972.
- [5] H.M. Tan, A. Moet, A. Hiltner, E. Baer, *Macromolecules*. 16 (1983) 28-34.
- [6] A. Coniglio, H.E. Stanley, W. Klein, *Phys. Rev. Lett.* 42 (1979) 518-522.
- [7] G.T. Feke, W. Prins, *Macromolecules*. 7 (1974) 527-530.
- [8] D.J. Lin, K. Beltsios, C.L. Chang, L.P. Cheng, *J. Polym. Sci. B: Polym. Phys.* 41 (2003) 1578-1588.
- [9] P. van de Witte, P.J. Dijkstra, J.W.A. van den Berg, J. Feijen, *J. Membr. Sci.* 117 (1996) 1-31.
- [10] J.S. Andrew, D.R. Clarke, *Langmuir*. 24 (2008) 670-672.
- [11] J.C. Jansen, M. Macchione, E. Drioli, *J. Membr. Sci.* 255, (2005) 167-180.
- [12] L. Shen, Y.H. Song, Y.J. Qian, F. Qiao, J. L. Zhang, Q. Zheng, *Chinese J. Polym. Sci.* 26 (2008) 639-644.
- [13] K. Ogasawara, T. Nakajima, K. Yamaura, S. Matsuzawa, *Colloid & Polym. Sci.* 254 (1976) 553-558.
- [14] L. Scanu, G.W. Roberts, J.M. DeSimone, S. Khan, *AIP Conf. Proc.* 1027, (2008) 360-363.
- [15] L.P. Cheng, D.J. Lin, C.H. Shih, A.H. Dwan, C.C. Gryte, *J. Polym. Sci. B: Polym. Phys.* 37, (1999) 2079-2092.
- [16] J.J. van Aartsen, *Eur. Polym. J.* 6 (1970) 919-924.
- [17] B. Zhou, A.C. Powell, *J. Membr. Sci.* 268, (2006) 150-164.
- [18] R. Gregorio, D. Sousa Borges, *Polymer*. 49 (2008) 4009-4016.
- [19] W. Ma, J. Zhang, X. Wang, *Appl. Surf. Sci.* 253 (2007) 8377-8388.
- [20] J.D. Mendelsohn, C.J. Barrett, V.V. Chan, A.J. Pal, A.M. Mayes, M.F. Rubner, *Langmuir*. 16 (2000) 5017-5023.